Effects of isotopic disorder on the Raman spectra of crystals: Theory and *ab initio* calculations for diamond and germanium

Nathalie Vast*
CEA–Centre d'Etudes de Bruyères, 91680 Bruyères Le Châtel, France

Stefano Baroni†
SISSA–Scuola Internazionale Superiore di Studi Avanzati and INFM–Istituto Nazionale per la Fisica della Materia, Via Beirut 2-4, 34014 Trieste, Italy

(Received 14 October 1999)

We present a method to study the effects of isotopic composition on the Raman spectra of crystals, in which disorder is treated *exactly* without resorting to any kind of mean-field approximation. The Raman cross section is expressed in terms of a suitable diagonal element of the vibrational Green's function, which is accurately and efficiently calculated using the recursion technique. This method can be used in conjunction with both semiempirical lattice-dynamical models and with first-principles interatomic force constants. We have applied our technique to diamond and germanium using the most accurate interatomic force constants presently available, obtained from density-functional perturbation theory. Our method correctly reproduces the light scattering in diamond—where isotopic effects dominates over the anharmonic ones—as well as in germanium, where anharmonic effects are larger.

I. INTRODUCTION

The striking successes met by the quantum theory of solids over the past 70 years are mostly due to a careful exploitation of the symmetry properties displayed by crystals because of translational invariance. The effects of isotopic composition on the vibrational spectrum of an otherwise perfect crystal are possibly the simplest manifestation of the phenomena which occur when translational invariance is broken by disorder. From a theoretical point of view, the study of these effects is particularly appealing because disorder does not affect the interactions between atoms—which can therefore be calculated with high accuracy using techniques appropriate for periodic systems—but only the mass distribution in the dynamical matrix. On the experimental side, the optical properties of isotopically enriched semiconductor samples, particularly germanium samples, have recently received a considerable attention motivated and triggered by the ability to separate and to alloy different isotopes of a given element and to produce either isotopically pure or intentionally disordered high-purity crystals.[1]

The effects of substitutional disorder on the vibrational properties of crystals are usually treated by some kind of approximation aimed at defining an effective periodic dynamical matrix whose resolvent is the average Green's function of the system (i.e., the Green's function averaged over the different realization of the disorder).[2] The simplest of such approximations is the virtual crystal approximation (VCA) in which the fluctuations in the variables which determine the randomness in the system (the nuclear masses in the case of isotopic disorder) are simply neglected and these variables replaced by their average value. Several improvements exist over the VCA—such as, notably, the coherent-potential approximation (CPA)—in which fluctuations in the mass distribution are treated in the mean-field approximation at different levels of sophistication.[3]

In this paper we show how the effects of isotopic disorder on the Raman spectra of crystals can be treated essentially without any approximations, besides those used for the calculation of the interatomic force constants. To this end, we first express the Raman cross section in terms of the vibrational Green's function of the crystal, and then we calculate the latter by using the recursion method. Section II contains our theoretical formulation, while in Sec. II we present the results that we have obtained by applying our theory to diamond and germanium crystals, and using *ab initio* interatomic force constants.

II. THEORY

In the specific case of the Raman spectrum and in the adiabatic approximation, the cross section for the nonresonant inelastic scattering of a photon polarized along the $\boldsymbol{\epsilon}_{in}$ direction to a final state polarized along the $\boldsymbol{\epsilon}_{out}$ direction is given by

$$\sigma(\omega) \propto \sum_{if} P(E_i)\,\delta(\omega - E_f + E_i) \times \left| \int \Phi_f^*(\boldsymbol{u})\, \boldsymbol{\epsilon}_{out}^* \cdot \boldsymbol{\chi}(\boldsymbol{u}) \cdot \boldsymbol{\epsilon}_{in} \Phi_i(\boldsymbol{u})\, d\boldsymbol{u} \right|^2, \qquad (1)$$

where E_i and E_f indicate the energies of the initial (i) and of the final (f) vibrational states of the system, Φ_i and Φ_f the corresponding wave functions, P the thermal distribution of initial states, $\boldsymbol{u}$ the vibrational coordinates, and $\boldsymbol{\chi}(\boldsymbol{u})$ is the static electronic polarizability tensor of the system expressed as a function of the nuclear coordinates. Let us assume that the system is initially in its ground state ($T=0$). By expanding $\boldsymbol{\chi}$ in powers of $\boldsymbol{u}$ up to linear order and making the harmonic approximation for the lattice vibrations, the cross section reads

$$\sigma(\omega) \propto \sum_{\nu} \delta(\omega-\omega_{\nu}) \left| \sum_{l} \chi'_{l} \xi_{l,\nu} \langle \Phi_{\nu} | Q_{\nu} | \Phi_0 \rangle \right|^2, \quad (2)$$

where $|\Phi_0\rangle$ is the vibrational ground state of the system, $|\Phi_{\nu}\rangle$ the state with one phonon emitted in the νth normal mode, Q_{ν} and $\xi_{l,\nu}$ the corresponding normal coordinate and displacement pattern ($\xi_{l,\nu} \equiv \partial u_l / \partial Q_{\nu}$), and $\chi'_l = \partial [\boldsymbol{\epsilon}^*_{\rm out} \cdot \boldsymbol{\chi}(\boldsymbol{u}) \cdot \boldsymbol{\epsilon}_{\rm in}] / \partial u_l$. In Eq. (2) and in the following the l subscript labels an individual nuclear coordinate [as specified by the position of the unit cell $\boldsymbol{R}$, by the atomic position within the unit cell s, and by direction of the displacement from equilibrium α: $u_l \equiv u_{s,\alpha}(\boldsymbol{R})$]. Taking into account that the matrix element of Q_{ν} is proportional to $(2\omega_{\nu})^{-1/2}$, Eq. (2) can be recast into the very simple form:

$$\sigma(\omega) \propto \frac{1}{\pi} \mathrm{Im} \sum_{ll'} \chi'^{*}_{l} G_{ll'}(\omega) \chi'_{l'}, \quad (3)$$

where $\boldsymbol{G} = (\boldsymbol{M}\omega^2 - \boldsymbol{K})^{-1}$ is the vibrational Green's function of the system, $\boldsymbol{K}$ the matrix of the interatomic force constants, and $\boldsymbol{M}$ is the (diagonal) matrix which specifies the atomic mass distribution. In Eq. (3) it is assumed that ω has an infinitesimal negative imaginary part. Equation (3) states that the nonresonant Raman cross section is essentially given by the imaginary part of a certain diagonal element of the vibrational Green's function, calculated with respect to the vector of the partial derivatives of the electronic polarizability with respect to all the nuclear displacements.

In the adiabatic approximation, the electronic ground-state wave function of a crystal is lattice periodic and is unaffected by isotopic disorder. Because of periodicity, $\chi'_l \equiv \chi'_{s,\alpha}(\boldsymbol{R})$ cannot depend on the position of the unit cell $\boldsymbol{R}$. In the absence of isotopic disorder, $\boldsymbol{G}(\omega)$ is also lattice periodic and the density of states (DOS) projected over a lattice periodic vector can only be nonvanishing if ω coincides with one of the zone-center vibrational frequencies of the system. Thus, we recover the well known selection rule that, in the absence of disorder (and ignoring anharmonic effects) Raman lines are delta functions centered at $\boldsymbol{q}=\boldsymbol{0}$ vibrational frequencies (further selection rules may obviously hold because of point symmetry). Isotopic disorder is often said to allow lattice vibrations with a finite wave vector to be excited in the scattering process. Inspection of Eq. (3) suggests a complementary picture: the momentum transferred by (visible or infrared) light to the crystal is always vanishingly small, as dictated by kinematic selection rules or, equivalently, by the fact that χ' is lattice periodic. The broadening of the Raman lines may be seen as due to the fact that in the presence of disorder *all* the vibrational eigenstates have a nonvanishing component over the lattice-periodic χ' vector. Of course, in the weak-disorder limit, it is expected that only those vibrational eigenstates whose frequency is close to a Raman-active mode of the virtual crystal may have an appreciable projection over χ', so that in this case Raman spectra still consist of well defined individual lines which are broadened by disorder. For crystals with the diamond structure, point symmetry dictates that

$$\frac{\partial \chi_{\alpha\beta}}{\partial u_{s,\gamma}(\mathbf{R})} = \mathrm{const} \times (-1)^s \times |\epsilon_{\alpha\beta\gamma}|, \quad (4)$$

where Greek letters indicate Cartesian coordinates, $s \equiv \{1,2\}$ indicates the two equivalent atomic sites in the unit cell, and $\boldsymbol{\epsilon}$ is the Levi-Civita totally antisymmetric unit tensor.[4] According to Eq. (4), if the incoming light is polarized, say, along the x axis and the scattered photon is observed along the y direction, then χ'_l is proportional to the displacement vector of a zone-center optical phonon polarized along the z direction. Equation (3) states that the Raman cross section is given by the diagonal matrix element of the vibrational Green's function of the disordered crystal, calculated with respect to this lattice periodic vector. The most efficient method known to date to calculate diagonal matrix elements of this form is the Haydock's recursion method.[5]

In order to apply the recursion method to the calculation of the matrix element, Eq. (3), we first rewrite it as

$$\sigma(\omega) \propto \mathrm{Im} \left\langle \xi_0 \left| \frac{1}{\omega^2 - \overline{\boldsymbol{K}}} \right| \xi_0 \right\rangle, \quad (5)$$

where

$$\overline{\boldsymbol{K}} = \boldsymbol{M}^{-1/2} \boldsymbol{K} \boldsymbol{M}^{-1/2}, \quad (6)$$

and

$$|\xi_0\rangle = \boldsymbol{M}^{-1/2} |\chi'\rangle. \quad (7)$$

Application of standard techniques[5] leads to the continued-fraction expansion

$$\sigma(\omega) \propto \mathrm{Im} \cfrac{1}{\omega^2 - a_0 - \cfrac{b_1^2}{\omega^2 - a_1 - \cfrac{b_2^2}{\ddots}}}, \quad (8)$$

where the a and b coefficients are given by the recursion chain

$$|\xi_{-1}\rangle = 0,$$

$$b_n |\xi_n\rangle = (\overline{\boldsymbol{K}} - a_{n-1}) |\xi_{n-1}\rangle - b_{n-1} |\xi_{n-2}\rangle, \quad (9)$$

and

$$a_n = \langle \xi_n | \overline{\boldsymbol{K}} | \xi_n \rangle, \quad b_n = \langle \xi_n | \overline{\boldsymbol{K}} | \xi_{n-1} \rangle. \quad (10)$$

The recursion method is almost invariably used as a *real-space* technique, mainly to calculate the local density of states and related properties in disordered systems.[6] However, this method can be applied as well in any representation where the matrix-vector product appearing in Eq. (9)—which is the time-consuming step of the algorithm—can be efficiently calculated. In the present case, this is most conveniently done using spectral techniques. In fact, $\overline{\boldsymbol{K}}$ is the product of matrices which are either diagonal in real space ($\boldsymbol{M}$), or block-diagonal in reciprocal space ($\boldsymbol{K}$). The recursion vectors can be kept stored in either representation, and the matrix-vector products performed in the representation where the matrix is (block) diagonal. The transformation from one representation to the other is most efficiently done using fast Fourier transform techniques (FFT). In this way, once the force-constant matrices $\boldsymbol{K}(\mathbf{q})$ are calculated on a

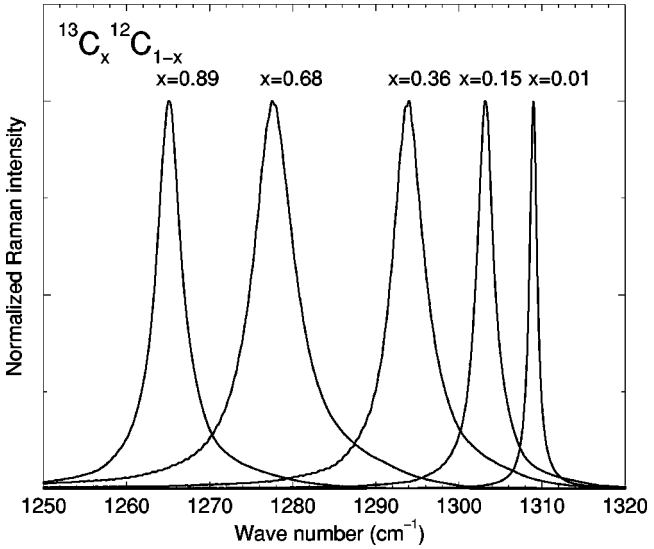

FIG. 1. Raman intensities in diamond, calculated for different isotopic compositions.

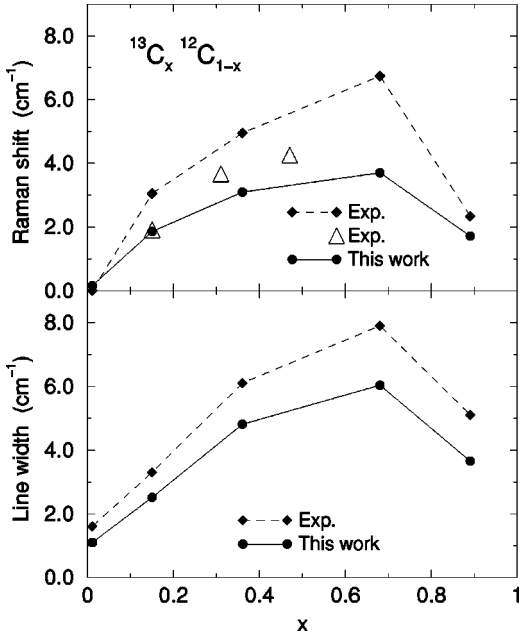

FIG. 2. Raman shift (upper panel) and linewidth (lower panel) in diamond as functions of ^{13}C. Experimental data are from Ref. 7 (filled diamonds) and Ref. 22 (triangles). The resolution of the spectrometer is included in the experimental linewidth and has been estimated to 1.8 cm^{-1}.[9]

regular mesh of $\boldsymbol{q}$ vectors (using either a semiempirical model or first-principles techniques) the calculation of the Raman cross section using Eqs. (8)–(10) can be easily carried out.

III. RESULTS

We have applied the formalism presented above to diamond and germanium for which a good deal of experimental information is available. Natural diamond form a binary *isotopic alloy* composed of 98.9% of ^{12}C and 1.1% of ^{13}C. The Raman spectrum of artificially ^{13}C-enriched samples has been determined for different concentrations ^{13}C.[7–9] Natural germanium has a more complex composition with 22% of ^{70}Ge, 28% of ^{72}Ge, 8% of ^{73}Ge, 35% of ^{74}Ge, and 6% of ^{76}Ge.[1] The Raman spectra of pure isotopes as well as that of the binary alloy $^{70}Ge_{0.5}\,^{76}Ge_{0.5}$ have also been determined.[1,10–12]

The force-constant matrices $\boldsymbol{K}(\mathbf{q})$ have been calculated using density functional perturbation theory (DFPT) (Ref. 13) on a regular (8,8,8) grid of $\boldsymbol{q}$ points in the reciprocal space of the face-centered cubic lattice. These matrices have then been Fourier-interpolated onto a (32,32,32) grid, following the same procedure as in Ref. 14. The real-space image of such a grid is a supercell containing $2\times32^3 = 65536$ atoms. We have used the plane-wave pseudopotential method with norm-conserving pseudopotentials from Ref. 15 for C and Ref. 16 for Ge. Plane waves up to a kinetic-energy cutoff of 40 and 16 Ry were used for C and Ge, respectively, and the Brillouin-zone integrations were performed using 10 special $\boldsymbol{k}$ points. All the calculations were done at the theoretical equilibrium crystal volume, corresponding to 11.1 and 43.7 Å^3 for diamond and germanium, respectively, and the slight dependence of the volume on the isotopic composition[17] has been neglected. The resulting optical frequencies at zone center are 1309 and 303 cm^{-1} in diamond and germanium, respectively—when calculated with a value of the mass equal to the natural average—to be compared with the experimental values of 1331 (Ref. 18) and 304 (Ref. 19) cm^{-1}.

The recursion chain, Eqs. (9),(10), has been implemented by generating a random distribution of nuclear masses in the above mentioned supercell, corresponding to any given isotopic composition. The chain was truncated after 600 steps of recursion, and the results averaged over 5–10 independent mass distributions corresponding to a same isotopic composition. *Ghost* states may appear while generating such long chains[20] due to the numerical loss of orthogonality among different recursion vectors. The existence of these ghosts, however, does not affect the value of the Green's function we are interested in, as it was explicitly verified by reorthogonalizing the chain vectors. Anharmonic effects on the Raman line shape were taken into account semi-empirically by evaluating the Green's function at the complex frequency $\omega - i\Gamma_{\mathrm{anh}}$, where Γ_{anh} is the inverse lifetime of the LTO zone-center phonon, as determined theoretically using third-order DFPT.[21]

In Fig. 1 we display the Raman lines calculated in diamond for different isotopic compositions. The main effect of the variation of the ^{13}C concentration x is that the position of the peak is inversely proportional to the square root of the average mass, as predicted by the VCA. As x varies, the width of the peaks changes from a minimum corresponding to the two pure-isotope limits ($x=0$ and $x=1$)—where only anharmonic effects contribute to the phonon lifetime—to a maximum occurring near $x\approx0.7$ where effects of disorder are the largest. In Fig. 2 we display the dependence of the disorder-induced frequency shift and linewidth upon ^{13}C concentration. Formally these two quantities coincide with the real and imaginary parts of the disorder-induced phonon self-energy. The former is obtained by subtracting the prediction of the VCA from the position of the maximum of the line, whereas the latter is increased by twice the theoretical anharmonic inverse lifetime in order to compare with experi-

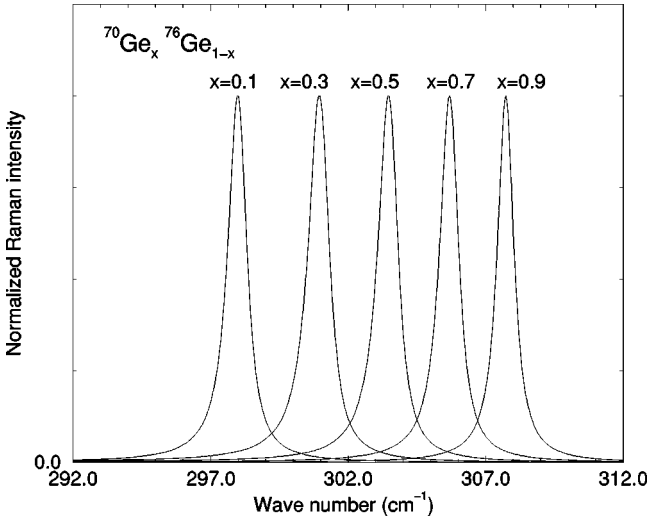

FIG. 3. Raman intensities in $^{76}Ge_x\,^{70}Ge_{1-x}$, calculated for different isotopic compositions x.

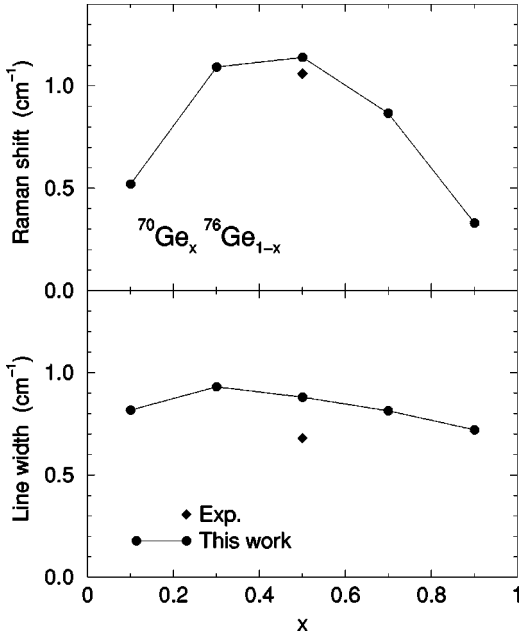

FIG. 4. Raman shift (upper panel) and line width (lower panel) in $^{76}Ge_x\,^{70}Ge_{1-x}$ as functions of x. Experimental data are from Ref. 11. Pure ^{70}Ge and ^{76}Ge have a theoretical anharmonic linewidth of 0.67 cm^{-1}.[21]

ments. We see that, while the accuracy of our calculated force constants limits the absolute precision of our predictions to ≈ 20 cm^{-1} (which is the error in the prediction of the zone-center optical frequency at natural isotopic composition), the dependence upon composition of the disorder-induced frequency shifts and linewidths are very well reproduced by our calculations. In particular, in agreement with experiments[7] and with previous calculations based on the CPA and on a semiempirical force field,[8] the maximum of the disorder-induced self-energy is shifted towards heavier average masses ($x \approx 0.7$). The scattering probability is roughly proportional to the vibrational density of states and the self-energy is enhanced at lower (higher) frequency when the perturbing atoms are ^{13}C (^{12}C).[8,22] Therefore, maximum effects are found at a composition for which the average mass is heavier than that corresponding to $x=0.5$, for which the mass disorder is maximum (Fig. 2). We note that, at variance with our data which are obtained treating disorder exactly, the bowing of the Raman shift curve is strongly reduced when the CPA is used in conjunction with *ab initio* interatomic force constants.[22]

The self-energy predicted by our calculations is systematically smaller than observed experimentally by Raman scattering. Self-energy effects are relatively large in diamond because of the large density of states available for scattering LTO_Γ phonons off the zone center.[8] This large density of states is due to the overbending of the phonon dispersion near the zone center.[23,24] Actually, first-principles calculations predict a maximum of the phonon DOS more than 20 cm^{-1} above the LTO_Γ frequency,[24] whereas according to second-order Raman experiments,[25] this maximum should be located only a few cm^{-1} above. This fact seems to be supported by recent inelastic x-ray scattering measurements of the phonon dispersions in diamond[26] which display a smaller overbending than predicted by first-principles calculations. We conclude that first-principles calculations slightly overestimate the overbending of phonon dispersions at zone center in diamond, and they also underestimate the vibrational DOS near the LTO_Γ frequency.

However, increasing the DOS near the LTO_Γ frequency has little effects—when using the CPA—on the real part of the self-energy but increases the imaginary part by a factor as large as 2.[9] Then we believe that both the inaccuracy of calculated DOS and the experimental resolution—estimated to be ≈ 1.8 cm^{-1} (Ref. 9)—do explain the discrepancy between the theoretical and experimental linewidths, but not the whole discrepancy on the Raman shifts.

So far, we have compared our theoretical Raman shift and broadening to the Raman-scattering experiment of Ref. 7. A recent investigation of the isotopic effects on the frequency shift both by cathodoluminescence and Raman measurements[22] estimates the value of 0.5 meV (4 cm^{-1}) as an upper bound for the shift of the LTO_Γ frequency within the $[x=0, x=0.5]$ concentration range for the $^{13}C_x\,^{12}C_{1-x}$. Our theoretical Raman shifts are in better agreement with those measurements (Fig. 2).

In Figs. 3 and 4 we display the shape of the Raman peaks and the magnitude of the disorder-induced frequency shifts and linewidths, as calculated for different isotopic compositions in $^{76}Ge_x\,^{70}Ge_{1-x}$. In this case the effects of disorder are of the order of 1 cm^{-1} and are much smaller than in diamond, due to the fact that the Γ_{LTO} phonon lies at the edge of the optical band, where the vibrational DOS vanishes.[1] Even though the comparison of our results with experiments is for this reason extremely difficult and to some extent even questionable, our calculations are indeed able to describe some fine details of the observed line shape to a very high accuracy. This is illustrated in Fig. 5 which shows how the two shoulders in the low-energy tail of the Raman peak in $^{76}Ge_{0.5}\,^{70}Ge_{0.5}$, corresponding to the L_{TO} and X_{TO} critical points of the density of states[12] are well reproduced by our calculations.

In the germanium alloy the theoretical Raman shift is in very close—and somewhat fortuitous—agreement with the sole measurement made at $x \approx 0.5$ (Fig. 4). Our theoretical results predict that the maximal effect is expected at that

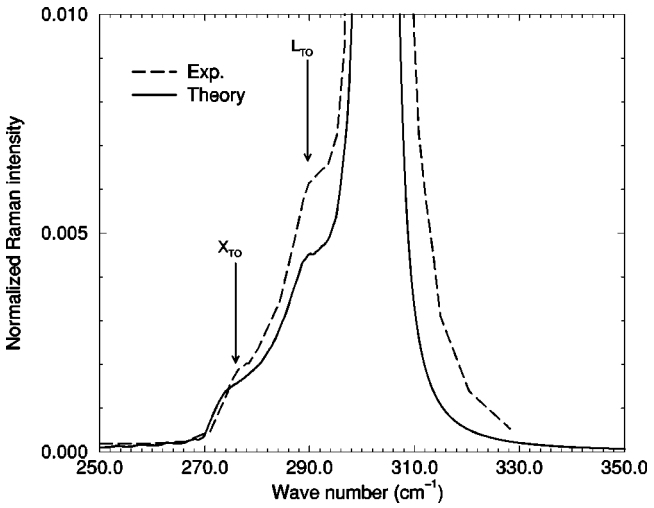

FIG. 5. Low-energy tail of the Raman line of $^{76}Ge_{0.5}{}^{70}Ge_{0.5}$. The frequencies of the L_{TO} and X_{TO} critical points are marked by an arrow. Experiment is from Refs. 11,12. The theoretical peak has been shifted so that the maximum of the peak coincides with the experimental value (304.5 cm^{-1}).

composition although the curve is not symmetric with respect to $x=0.5$.

The linewidth of natural germanium is small and therefore difficult to measure. Different values have recently been reported, ranging from 0.51 (Ref. 27) to 0.64 (Ref. 28) and to 0.97 cm^{-1},[10] while the theoretical estimate for the purely anharmonic contribution is 0.67 cm^{-1}.[21] The theoretical broadening in the binary alloys is also small over the whole range of concentrations (Fig. 4), and it is predicted to increase with respect to the purely anharmonic width over the whole range of concentration. However, the smallness of this effect does not allow us to make any quantitative meaningful prediction about its dependence upon x. For $x\approx 0.5$, the linewidth reaches ≈ 0.9 which is ≈ 0.2 cm^{-1} larger than the pure anharmonic broadening occurring in the nondisordered case. This figure is an order of magnitude larger than the experimental value, as a 0.02 cm^{-1} broadening is reported.[1] This discrepancy in the theoretical and experimental linewidths also appears on Fig. 5, where the experimental low-energy tail of the Raman line is slightly broader than the theoretical one.

IV. CONCLUSIONS

In conclusion, we present a theoretical method to investigate the effects of isotopic disorder on the lattice dynamics of crystals, which does not rely on any kind of mean-field approximations. For diamond, our results are in reasonable agreement with experiments although they depend sensitively on the calculated vibrational DOS at the LTO_Γ frequency, which is presumably underestimated by the present DFPT calculations. The effects for Ge are much weaker. Nevertheless the agreement between our results and experiment is still very satisfactory also in this case.

ACKNOWLEDGMENTS

We would like to acknowledge useful discussions with J.M. Besson, A. Debernardi, P. Giannozzi, Ph. Pruzan, and T. Ruf. Special thanks are due to M. Cardona for illuminating discussions and continuous encouragement. Part of this work has been done while one of us (S.B.) was at the *Centre Europeéen de Calcul Atomique et Moléculaire* (CECAM) in Lyon.

*Leaving present address for: CEA-Laboratoire des Solides Irradiés, 91128 Palaiseau, France. Electronic address: vast@bruyeres.cea.fr

†Electronic address: baroni@sissa.it

[1] For a review on the effects of isotopic disorder on the vibrational properties of (possibly isotopically engineered) materials, see, e.g., M. Cardona, P. Etchegoin, H.D. Fuchs, and P. Molinas-Mata, J. Phys. C **5**, A61 (1993).

[2] For a review on the theoretical tools currently used for dealing with substitutionally disordered systems, see, e.g., R.J. Elliot, J.A. Krumnansl, and P.L. Leath, Rev. Mod. Phys. **46**, 465 (1974).

[3] E.N. Economou, *Green's Function in Quantum Physics* (Springer-Verlag, Berlin, 1983).

[4] S. Baroni and R. Resta, Phys. Rev. B **33**, 5969 (1986).

[5] R. Haydock, Solid State Phys. **35**, 215.

[6] A similar approach for calculating the electronic spectral density in substitutional semiconductor alloys has been followed, e.g., in K.C. Hass, L.C. Davis, and A. Zunger, Phys. Rev. B **42**, 3757 (1990).

[7] R.M. Chrenko, J. Appl. Phys. **63**, 5873 (1988).

[8] K.C. Hass, M.A. Tamor, T.R. Anthony, and W.F. Banholzer, Phys. Rev. B **45**, 7171 (1992).

[9] J. Spitzer, P. Etchgoin, M. Cardona, T.R. Anthony, and W.F. Banholzer, Solid State Commun. **88**, 509 (1993).

[10] H.D. Fuchs, C.H. Grein, C. Thomsen, M. Cardona, W.L. Hansen, E.E. Haller, and K. Itoh, Phys. Rev. B **43**, 4835 (1991).

[11] P. Etchgoin, H.D. Fuchs, J. Weber, M. Cardona, L. Pintschovius, and N. Pyka, Phys. Rev. B **48**, 12 661 (1993).

[12] H.D. Fuchs, P. Etchegoin, M. Cardona, K. Itoh, and E.E. Haller, Phys. Rev. Lett. **70**, 1715 (1993).

[13] S. Baroni, P. Giannozzi, and A. Testa, Phys. Rev. Lett. **58**, 1861 (1987).

[14] P. Giannozzi, S. de Gironcoli, P. Pavone, and S. Baroni, Phys. Rev. B **43**, 7231 (1991).

[15] K. Mäder and S. Baroni, Phys. Rev. B **55**, 9649 (1997).

[16] S. Baroni, P. Pavone, P. Giannozzi, S. de Gironcoli, and E. Molinari, in *Light Scattering in Semiconductor Structure and Superlattices*, Vol. 273 of *NATO Advanced Study Institute, Series B: Physics*, edited by D.J. Lockwood and J.F. Young (Plenum Press, New York, 1991).

[17] P. Pavone and S. Baroni, Solid State Commun. **90**, 295 (1994).

[18] J.L. Warren, J.L. Yarnell, G. Dolling, and R.A. Cowley, Phys. Rev. **158**, 805 (1967).

[19] G. Nilsson and G. Nelin, Phys. Rev. B **3**, 364 (1971).

[20] R. Haydock, *The Recusion Method and its Applications* (Springer Verlag, Berlin, 1985), p. 8.

[21] A. Debernardi, S. Baroni, and E. Molinari, Phys. Rev. Lett. **75**, 1819 (1995).

[22] T. Ruf, M. Cardona, H. Sternschulte, S. Wahl, K. Thonke, R. Sauer, P. Pavone, and T.R. Anthony, Solid State Commun. **105**, 311 (1998).

[23] R. Tubino and J.L. Birman, Phys. Rev. Lett. **35**, 670 (1975); Phys. Rev. B **15**, 5843 (1977).
[24] W. Windl, P. Pavone, K. Karch, O. Schütt, D. Strauch, P. Giannozzi, and S. Baroni, Phys. Rev. B **48**, 3164 (1993).
[25] M.A. Washington and H.Z. Cummins, Phys. Rev. B **15**, 5840 (1977).
[26] M. Schwoerer-Böhning, A.T. Macrander, and D. Arms, Phys. Rev. Lett. **80**, 5572 (1998).
[27] C. Ulrich, E. Anastassakis, K. Syassen, A. Debernardi, and M. Cardona, Phys. Rev. Lett. **78**, 1283 (1997).
[28] J.M. Zhang, M. Giehler, A. Göbel, T. Ruf, M. Cardona, E.E. Haller, and K. Itoh, Phys. Rev. B **57**, 1 (1998).